Characterizing the Properties of the N7,N9-Dimethylguaninium Chloride Ion Pairs: Prospecting for the Design of a Novel Ionic Liquid

Dianxiang Xing,*,†,‡ Yuxiang Bu,*,† and Xuejie Tan‡

Institute of Theoretical Chemistry, Shandong University, Jinan, 250100, People's Republic of China, and School of Chemical Engineering, Shandong Institute of Light Industry, Jinan, 250353, People's Republic of China

Received: July 31, 2007; In Final Form: October 15, 2007

The structures, infrared spectra, and electronic properties of the N7,N9-dimethylguaninium chloride have been studied. The interaction of one cation with one to four Cl anions and one Cl anion with two cations were investigated. Fifteen stable conformers are obtained. It is found that there are four acidic regions in the vicinity of the guaninium cations. In these regions, the cation could H-bond with one to three Cl anions but no more than three nearest anions. One Cl anion could H-bond with two cations. Additionally, evidence of a Cl···π interaction between the anion and cation is observed. Among these structures, one cation interaction with two anions and two cations interaction with one anion have the larger interaction energies than the other series. Natural bond orbital analyses and molecular orbitals reveal that the charge transfer from anion(s) to the cation(s) occurs mainly through either the $Cl^{lp} \rightarrow \sigma^*_{C-H}$, $Cl^{lp} \rightarrow \sigma^*_{N-H}$, or $Cl^{lp} \rightarrow \pi^*_{C8-N7}$ interactions. The interaction between Cl and $\sigma^*_{(C/N-H)}$ or π^*_{C-N} produces a small bond order. This indicates that the Cl···H (Cl···π) interaction exhibits a weak covalent character and suggests a strong ionic H-bond (Cl···π bond). What's more, formation of Cl···H/Cl···π bond decreases the bond order of the associated C/N−H bond or C^8-N^7 bond. In addition, examination of vibrational spectrum of each conformer explains the origin of H-bonding character.

Introduction

Room-temperature ionic liquids (RTILs) are a relatively new class of solvents that have attracted increasing attention over the past few years. Basically, RTILs are salts that have melting points at or below room temperature. Most typically, they are composed of a large organic cation and a weakly coordinating inorganic anion. Since they are salts, they have high thermal stability, ionic conductivity, solubility power, nonflammability, and negligible vapor pressures.[1,2] These traits have attracted a great deal of interest toward their application as green, recyclable alternatives to conventional volatile in organic reaction. What is more, the unique properties of ILs also open up the possibility of realizing a vast range of novel applications such as in electrochemistry[3] and biocatalysis.[4] There also has been a great deal of interest in the application of the ILs as better heat-transfer fluids and lubricants.[5] The discovery of magnetic ILs has further broadened their applications.[6,7] It has been recently established that the outcome of organic reactions can be controlled by the choice of IL[8] and that both the anion and cation can interact specifically with catalysts or substrates.[9−13] ILs are also interesting because of their other useful and intriguing physicochemical properties. Wilkes et al. first reported ambient-temperature ILs based on the 1-alkyl-3-methylimidazolium cation in 1982.[14] Since then, many ILs containing a variety of cations and anions of different sizes have been synthesized to provide specific characteristics.

Although much attention has been paid to the study of the various applications, the design, and the properties of new ILs, at present, there is no way of determining a priori which particular ion pairing will produce the desired properties, and thus many groups are still devoted to develop the new, functionalized RTILs. In particular, two classes of RTILs have recently been developed. The first is based on the nitrogen-containing cations (e.g., imidazole and pyridine) and various inorganic anions;[15] the second is based on imidazolium cation and various amino acids anion.[16] In terms of the new RTILs, ionic constituents and the size of IL seem to be critical. Early work indicated that the anionic constituents of ILs may have a greater influence on their physical and chemical properties.[17] However, recent studies have shown that the cationic constituent of ILs is important to the thermal stability of the IL.[18,19] They observed that the bulkier cations[18] and dicationic salts[19] rather than monocationic salts vastly improved the thermal stability of ILs. Thus, a bulkier cation seems to be another crucial factor to be considered for the design of new ILs. Guanine, one of the five nucleic acids with a low symmetry and larger bulk than imidazole, seems to be an appropriate replacement for imidazole. What's more, the fact that a nucleic acidic base, as a fine inheritance, has the ability to store and transfer information through Watson−Crick base pairing has promoted us to design purine-containing cationic ILs that have some specific function to favor the biological synthesis. Herein, we report a novel compound based on N7,N9-dimethylated guanine that might be used as an IL.

For a new IL, it is essential to make a link between the structure and the physical properties that are controlled by the intermolecular interaction between ions.[20] The ability to predict the physicochemical properties of an unknown IL will depend on understanding the molecular-level interactions. Thus an important aspect of the ILs that needs to be further understood

* To whom correspondence should be addressed. E-mail: xdx@mail.sdu.edu.cn and byx@sdu.edu.cn.
† Shandong University.
‡ Shandong Institute of Light Industry.

10.1021/jp0760509 CCC: $40.75
Published on Web 12/13/2007

is the nature of the interaction among the ions present. Recently, ab initio molecular orbital (MO) calculation has been becoming a powerful tool for studying intermolecular interaction.[21] Recent ab initio calculations of small molecular clusters show that ab initio calculations provide sufficiently accurate interaction energies, if a reasonably large basis set and theoretical method are used.[22] Therefore, to obtain a deeper understanding of the fundamental molecular-level interactions occurring in an IL, we have performed an analysis of the gas-phase N7,N9-dimethylguaninium chloride ion pair ([dMG]Cl).

In this work, we first describe the interaction of one cation with one anion in detail to understand the condensed phase of an IL. Additionally, it is known that a superior method to understand the condensed phase of an IL is given by molecular dynamic simulations. However, it is somewhat difficult to perform simulation for the condensed phase of [dMG]Cl ion pair due to the absence of the indispensable experimental parameters of [dMG]Cl ion pair. Thus, to better describe the condensed phase and to bridge the gap between static electronic structure calculations and classical molecular dynamics simulations, we also performed calculations of larger clusters built from the interactions of one cation combined with one to four Cl anions and the interaction of one anion combined with two cations. The purpose of the present research is to explore, using quantum chemical methods, the structure and H-bonding in [dMG]Cl ion pair as well as the IR spectroscopy and electronic properties of [dMG]Cl ion pair. Here, the [dMG]Cl ion pair was not prepared synthetically. As a consequence, information on the structures of [dMG]Cl ion pair and its intrinsic properties are important not only fundamentally but also for various applications.

Computational Details

Density functional theory (DFT) calculations using B3LYP have been carried out as implemented in the GAUSSIAN 03 suit of programs.[24] The DFT method is known to yield reliable characteristics for H-bonding. Structures have been fully optimized at the B3LYP/6-31+G** (6-31+G*) level without symmetry constraints. Vibrational frequencies have been calculated at the same level to ensure that each stationary point was a real minimum. Final energy evaluation for all the optimized structures was done at the B3LYP/6-311++G** level of theory. The interaction energies of the ion pairs are defined as follows: $\Delta E = E(\text{ion pair}) - E(\text{cation}) - E(\text{anion})$. The energies do not include the basis set superposition errors (BSSE), since BSSE corrections only change the overall energies by less than 5 kcal/mol, which has no significant effect on the interaction energies in the ionic systems.[23] The interaction energies of [dMG]·*m*Cl ($m = 1-4$, the number of Cl anion) series are calculated at the B3LYP/6-311++G**//B3LYP/6-31+G** level. Those of the ion pairs formed by two cations with one anion ([2dMG]·Cl series) are calculated at the B3LYP/6-311++G**//B3LYP/6-31+G* level.

To examine the charge distribution and the nature of bonding interaction between the cation and the anion, natural bond orbital (NBO) analyses and Wiberg bond indexes of the considered conformers have been performed by using the methods in GAUSSIAN 03.[25] NBO analyses are carried out by examining all possible interactions between "filled" (donor) Lewis-type NBOs and "empty" (acceptor) non-Lewis NBOs and by estimating their energetic importance by second-order perturbation theory. Since these interactions lead to donation of occupancy from the localized NBOs of the idealized Lewis structure into the empty non-Lewis orbitals (and thus, to departure from the idealized Lewis structure description), they are referred to as "delocalization" corrections to the zeroth-order natural Lewis structure. For each donor NBO (*i*) and acceptor NBO (*j*), the stabilization energy *E*(2) associated with delocalization ("2e-stabilization") $i \rightarrow j$ is estimated as

$$E(2) = \Delta E_{ij} = n_i \frac{(F_{ij})^2}{\epsilon_j - \epsilon_i}$$

where $F(i,j)$ is the off-diagonal NBO Fock matrix element describing the donor−acceptor interaction, n_i is the donor orbital occupancy, and ϵ_i and ϵ_j are diagonal elements (orbital energies).

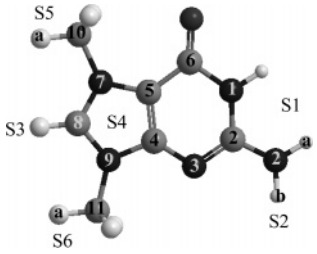

Figure 1. Atomic numbering of the isolated cation $[dMG]^+$. S1, S2, S3, S4, S5, and S6 denote the possible regions for Cl anions. Here, S4 means the region in the front or back of the C^8-H bond.

The atomic numbering of N7, N9-dimethyl guaninium ($[dMG]^+$) and the possible region for the Cl anion location are displayed in Figure 1. Four favorable regions S1, S2, S3, and S4 for the Cl anion are mainly taken into consideration. The notation used to denote the ion pairs is as follows: [dMG]·*m*Cl means a series of structures that formed by the interaction of one cation with one to four Cl anions (i.e., $m = 1-4$). [2dMG]·Cl stands for a series of structures formed by the interaction of two cations with one Cl anion. In [dMG]·mCl series, digit(s) in parentheses is (are) used to denote the favorable bonding regions of the Cl anion(s). For example, [dMG]·Cl(1) denotes that one Cl anion bonds with one cation in the region S1; [dMG]·2Cl(1.2) means that two Cl anions mainly interact with one cation in the regions S1 and S2, respectively.

Results and Discussion

1. Interaction of One Cation with One Cl Anion ([dMG]·Cl Series). *1.1. Geometries and Relative Stabilities.* The initial structures were determined by placing the Cl anion around the cation in "chemical intuitive" positions where interaction with hydrogen atoms (N−H···Cl, C−H···Cl)) or aromatic ring (π···Cl) of the N7,N9-dimethylguaninium cation was a possibility. Six structures were designed: four correspond to the interaction between N^1-H, N^2-H^a, N^2-H^b, or C^8-H of the cation and Cl anion; two correspond to the interaction between the aromatic ring and Cl anion. The optimization of N7,N9-dimethylguaninium chloride gave four conformers of the [dMG]·Cl ion pair (Figure 2.). These conformers will be identified as [dMG]·Cl-(1) (interaction through N^1-H and N^2-H^a simultaneously, region S1), [dMG]·Cl(2) (interaction through N^2-H^b, region S2), [dMG]·Cl(3) (interaction through C^8-H, region S3), and [dMG]·Cl(4) (Cl anion lies above the C^8-H bond of the cation, region S4), where the former three conformers in which the Cl anion remains roughly in-plane with the guaninium ring. Conformer [dMG]·Cl(4) is an exception, in which Cl anion is located above the imidazole ring of guaninium and more specifically above the C^8-H bond and positioned between the two N7 and N9-methyl hydrogen atoms. The position of the Cl anion in the stable structure is somewhat similar to the position of the Cl anion in the 1-methyl-3-metylimidazolium chloride

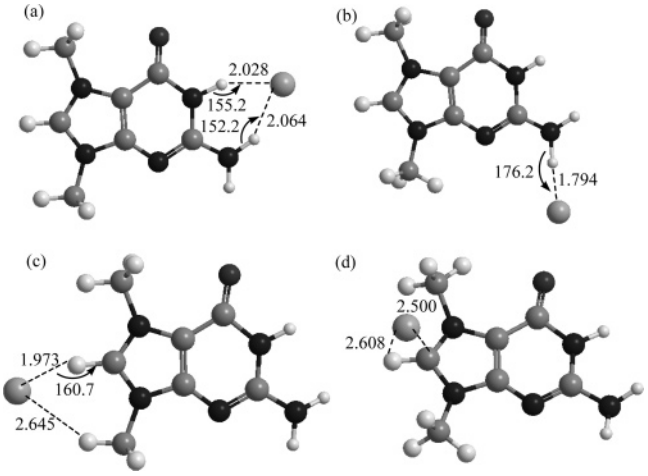

Figure 2. H-bonding interactions of the [dMG]·Cl series. All bond lengths are in angstroms, and angles are in degrees. (a) [dMG]·Cl(1); (b) [dMG]·Cl(2); (c) [dMG]·Cl(3); (d) [dMG]·Cl(4).

TABLE 1: Primary H-Bonding Parameters and Relative Stabilities of the Four [dMG]·Cl Ion Pairs[a]

	X−H[b]	$r_{H\cdots X}$	$r_{H\cdots Cl}$	$A_{X-H\cdots Cl}$[c]	*E*
$[dMG]^+$	N^1-H	1.016			
	N^2-H^{2a}	1.008			
	C^8-H	1.010			
[dMG]·Cl(1)	N^1-H	1.064	2.028	155.2	0
	N^2-H^{2a}	1.046	2.064	1.52.2	
[dMG]·Cl(2)	N^2-H^{2b}	1.116	1.794	176.2	13.53
[dMG]·Cl(3)	C^8-H	1.129	1.973	160.7	4.13
[dMG]·Cl(4)	C^8-H	1.076	2.608	72.3	2.32

[a] Energies in kcal/mol, distances in angstroms, angles in degrees. [b] X (hydrogen donor atom) is the ring atom (carbon or nitrogen atom) attached to hydrogen. [c] The bond angles of the H-bonding.

([C_1C_1im]Cl) ion pair,[26] where they also found total four conformers, in which three conformers have Cl anion lies in the plane of imidazolium and one has Cl position above the ring.

In the [dMG]·Cl ion pair, the cation−anion interaction is mainly through H-bonding as pointed out in imidazolium-based IL.[26,27] Thus the characterization of H-bonding is important. Here, we assign the interaction as a strong H-bond if H-bond length $r_{H\cdots Cl} < 2.30$ Å and a weak H-bond if $2.30 < r_{H\cdots Cl} < 2.75$ Å as literature reported[27a] (the sum of the van der Waals radii of Cl and H is 2.95 Å). The primary H-bond distances and the relative stabilities of the four conformers are summarized in Table 1. The detailed geometric characteristics are given in Table S1. As is shown in Table 1, these structures except for-[dMG]·Cl(4) ion pair, all form one strong H-bond (or two for the [dMG]·Cl(1)conformer, $r_{H\cdots Cl} < 2.0$ Å) to the N−H or C^8−H. Formation of H···Cl bond is expected to weaken the associated C/N−H bond, causing elongation of these bond distances and thereby lowering (red shifts) the associated C/N−H vibrational frequencies. These characteristics have been regarded as an unambiguous feature of the H-bond.[25a]

Among these four structures, the most stable conformer [dMG]·Cl(1) has the Cl anion positioned between N^1−H and N^2-H^{2a} but slightly moves toward N^1 (with $N^1H\cdots Cl$ and $N^2H^a\cdots Cl$ bond distances of 2.028 and 2.064 Å, respectively, Figure 2a). The Cl anion remains in-plane with the guaninium ring, since both $C^2-N^1-H\cdots Cl$ and $C^2-N^{2a}-H\cdots Cl$ dihedral angles are 0°. As expected, the bond lengths of N^1−H and N^2-H^a are lengthened by 0.048 and 0.038 Å, respectively, relative to those of the isolated cation. N^1−H is also the most acidic proton. Additionally, it is also found that the distances of the bonds around N^1 or N^2 atom (i.e., C^6-N^1, C^2-N^2, and N^2-H^b) are slightly shortened, while the other bonds remote to N^1 or N^2 are hardly affected by the H···Cl bond formation.

Lying about 2.32 kcal/mol higher in energy than the most stable one is [dMG]·Cl(4) (Figure 2d). Here, the Cl anion lies above the C^8−H bond, sitting closer to C^8 (length of $C^8\cdots Cl = 2.500$ Å) than the hydrogen (length of $H\cdots Cl = 2.608$ Å) and with a $H-C^8\cdots Cl$ angle of 72.3°. The interaction between the Cl anion and the ring slightly lengthens the C^8-N^9 and C^8-N^7 bonds and also the bond C^2-N^2 (Table S1). This structure differs significantly from all the other ion pairs in that no strong H-bonding interactions are present. The N9-methyl and N7-methyl hydrogen chloride distances (viz. $r_{C11Ha\cdots Cl}$ and $r_{C10Ha\cdots Cl}$) are 2.861 and 2.946 Å, respectively, indicating two very weak H-bonds. Additionally, there is the possibility of a Cl···π interaction for this ion pair since the guaninium cation is an electron-deficient aromatic ring and the Cl anion is an electron-rich monomer. If this is the case, the electron density of Cl anion might be transferred to the guaninium cation through the π bond. Further discussion would be provided in electronic properties below.

The [dMG]·Cl(3) (Figure 2c) is 4.13 kcal/mol higher in energy than the [dMG]·Cl(1). This structure forms a strong H-bond with C^8−H ($r_{H\cdots Cl} = 1.973$ Å) and a weak H-bond with N9-methyl hydrogen atom ($r_{H\cdots Cl} = 2.645$ Å). The Cl anion remains essentially in-plane with the guaninium ring, as the out-of-plane torsion angle $Cl-H-C^8-N^9$ is about −9.6°. The angle of C^8-H-Cl is 160.7°. Also, formation of $Cl\cdots H-C^8$ lengthens the C^8−H bond by ∼0.049 Å.

The [dMG]·Cl(2) (Figure 2b) is about 13.53 kcal/mol higher in energy than the [dMG]·Cl(1). In this conformer, Cl anion interacts with the cation through a strong H-bond with N^2-H^{2b} ($r_{H\cdots Cl} = 1.794$ Å, the angle $A_{Cl\cdots H-N2} = \sim 176.2°$). The Cl anion remains essentially in-plane with the guanininium ring ($D_{Cl-N2-C2-N1} = -8.9°$). Again, as anticipated, the associated N^2-H^{2b} bond is greatly lengthened by ∼0.106 Å upon the formation of H-bond. Here, the H^{2b} is the least acidic proton of the guaninium ring.

Besides the distance changes of Cl···H and X···H bonds in the four conformers, we also note that, when the Cl anion interacts with N−H bond, C^2-N^3 is slightly shortened, while the C^2-N^2 bond is slightly lengthened. However, when Cl anion interacts with a non-N−H bond, the changes of these two bonds are in contrast. However, all C═O bond distances are slightly elongated upon the formation of the ion pairs.

1.2. Interaction Energies. As is shown in Table 2, the interaction energies are very large due to electrostatic attraction between the cation and the anion, implying a negligible vapor pressure and high viscosity. The binding energies of these four ion pairs follow the order: [dMG]·Cl(1) > [dMG]·Cl(4) > [dMG]·Cl(3) > [dMG]·Cl(2)). This order reflects that, in the gas phase, the interaction of the Cl anion with the cation N^1-H and N^2-H^a is the most possible. However, the energy difference between the first three is not very large, and thus it seems that [dMG]·Cl(3) and [dMG]·Cl(4) are almost degenerate with the conformer [dMG]·Cl(1). On the other hand, the comparison of the binding energies with those of the 1-methyl-3-alkylimidazolium chloride ($C_nC_1$imCl) reveals that these values are slightly higher or comparable to 370 kJ/mol for [C_4C_1im]Cl[28] and 318.1−384.4 kJ/mol for [C_1C_1im]Cl ion pairs.[26] According to the binding energy, it may be deduced that the melting point and viscosity of the [dMG]Cl ion pair are comparable to that of the [C_4C_1im]Cl and [C_1C_1im]Cl ion pairs. Of course, we also note that more than one factor, such as the van der Waals

TABLE 2: Calculated Interaction Energies (ΔE) for N7,N9-Dimethylguaninium Chloride (Energies Are in kcal/mol)[a,b]

	ΔE		ΔE		ΔE		ΔE
[dMG]·Cl(1)	−92.8	[dMG]·2Cl(1.2)	−110.0	[dMG]·3Cl(1.2.3)	−112.6	[2dMG]·Cl-1	−130.7
[dMG]·Cl(2)	−79.3	[dMG]·2Cl(1.3)	−136.5	[dMG]·3Cl(1.3.6)	25.9	[2dMG]·Cl-2	−127.1
[dMG]·Cl(3)	−88.7	[dMG]·2Cl(2.3)	−123.8	[dMG]·3Cl(2.3.5)	−101.0	[2dMG]·Cl-3	−126.9
[dMG]·Cl(4)	−90.5	[dMG]·2Cl(4.4)	−110.8			[2dMG]·Cl-4	−127.5

[a] The interaction energies of the [dMG]·*m*Cl series are calculated at the B3LYP/6-311++G**//B3LYP/6-31+G** level; those of the [2dMG]Cl series are calculated at the B3LYP/6-311++G**//B3LYP/6-31+G* level. [b] The interaction energies of 1,3-dimethylimidazolium chloride ([C_1C_1im]Cl) varies from −318.1 to −384.4 kJ/mol depending on the position of Cl anion in the ion pair; values were taken from ref 26; while those of the stable conformer of [C_2C_1im]Cl and [C_4C_1im]Cl are −383.7 and −370.0 kJ/mol, respectively, values were taken from refs 27a and 27b, respectively.

TABLE 3: Primary C/N−H Vibrational Frequencies (cm^{-1}) for the Isolated Cation and Four Conformers of the [dMG]·Cl Series[a]

	X−H[b]	ν_s	$\nu_{as\ (N2-H)}$	$\Delta\nu$
$[dMG]^+$	N^1−H	3579.0		
	N^2−H^{2a}	3610.0	3739.6	
	C^8−H	3293.0		
[dMG]·Cl(1)	N^1−H	2737.5	3022.8	−841.5
	N^2−H			−716.8($\Delta\nu_{as}$)
	N^1−H	3597.0		18.0
[dMG]·Cl(2)	N^2−H^{2b}	1997.5	3641(N^2-H^{2a})	−1612.5($\Delta\nu_s$)
	C^8−H	3296.3		3.3
	N^1−H	3592.1		13.1
[dMG]·Cl(3)	N^2−H^{2a}	3601.4	3724.5	−9.6($\Delta\nu_s$), −15.1($\Delta\nu_{as}$)
	C^8−H	2558.6		−734.4
	N^1−H	3597.4		18.4
[dMG]·Cl(4)	N^2−H^{2a}	3589.1	3709.0	−21($\Delta\nu_s$), −30.6($\Delta\nu_{as}$)
	C^8−H	3320.6		27.6

[a] The frequencies are reported without correction.

interaction between the molecules, might contribute to the melting point of ILs. Here, this contribution could not be estimated and further investigation should be performed on larger clusters.

1.3. Properties of [dMG]·Cl Series. Chemists often ascribe the origin of X−H bond lengthening and the associated effects of a proper H-bond to the result of the electrostatic interaction[29−30] or hyperconjugation interaction.[25a] In the simplest explanation, electrostatic interaction causes X−H lengthening since the hydrogen acceptor atom pulls positive H closer to it and thus causes polarization of the X−H bond further, which not only increases the interaction but also increases the intensity of X−H stretching band in the IR. The red shift of vibrational frequency occurs because of weakening of the associated X−H bond. In the explanation of the hyperconjugation interaction, the stabilization is due to the overlap of the vacant σ^*_{X-H} bond with the filled MO of the hydrogen acceptor atom (usually the lone pair).[25a] Since the electron density transfers from the hydrogen acceptor atom to the σ^*_{X-H} antibonding orbital, the bond is weakened and lengthened. To better understand the nature of the bonding between the Cl anion and the cation, the vibrational frequencies, NBO analyses, and MOs were investigated.

1.3.1. IR Vibrations. Frequency analysis within the harmonic approximation has been performed for all the optimized structures. The selected vibrational frequencies of the ion pair and the isolated cation related to H-bonding are presented in Table 3. The IR spectroscopy of the isolated cation together with that of the four conformers is shown in Figure 3.

The computed C^8−H stretching vibrational mode for the isolated $[dMG]^+$ cation is 3293.6 cm^{-1}. The N−H stretching modes for the isolated $[dMG]^+$ cation are in the range of 3579.0−3739.6 cm^{-1}, which are three highest-energy stretching vibrations of the isolated cation. As is shown in Figure 3, they correspond to the antisymmetrical N^2−H (3739.6 cm^{-1}), the symmetrical N^2−H (3610.4 cm^{-1}), and a mode that is primarily the N^1−H (3579.0 cm^{-1}) stretching vibrations.

In comparisons with the isolated cation, three additional vibrations appear in the ion pair; they are mainly associated with the C/N−H···Cl interaction. However, these vibrations are not isolated but appear in combination modes, and the vibrational frequencies of C/N−H···Cl bond are small. Additionally, it can be seen from Figure 3 that the vibrational frequency of the C^6═O double bond in each conformer is slightly red-shifted relative to that in the isolated cation, which is in line with the changes of the C^6═O bond lengths mentioned above. The

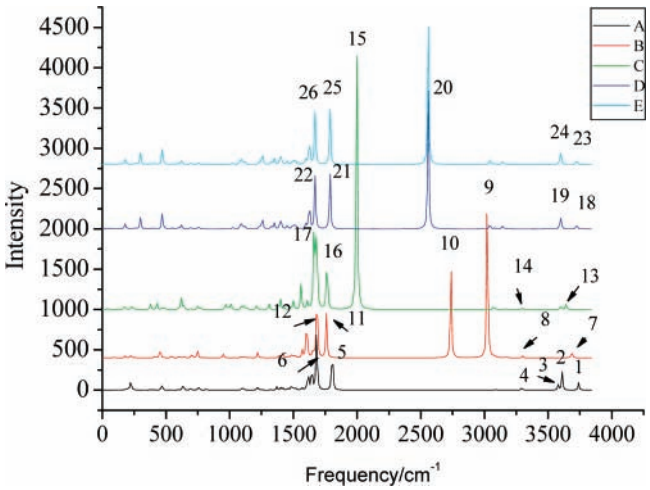

Figure 3. The primary vibration frequencies of the four ion pairs and the isolated cation. (A) $[dMG]^+$; (B) [dMG]·Cl(1); (C) [dMG]·Cl(2); (D) [dMG]·Cl(3); (E) [dMG]·Cl(4). Numbers denote the primary vibrational modes of the cation or ion pairs. The vibrational modes are as follows: 1, ν_{asN2}−H; 2, ν_{sN2}−H; 3, ν_{sN1}−H; 7, ν_{sN2}−Hb; 9, ν_{sN2}−Ha + ν_{sN1}−H; 10, ν_{sN1}−H + ν_{sN2}−Ha; 13, ν_{sN2}−Ha; 23, ν_{asN2}−H; 24, ν_{sN1}−H; 18, ν_{asN2}−H; 19, ν_{sN1}−H + ν_{sN2}−H; 15, ν_{sN2}−Hb; 4, 8, 14, and 20 are stretching vibrations of C^8−H. 5, 11, 25, 21, and 16 are stretching vibrations of C═O ($\nu_{sC6=O}$). 6, 12, 26, 22 and 17 are bending vibrations of N^2−H and N^1−H (τ_{N2-H} + τ_{N1-H}). In the conformers [dMG]·Cl(1), [dMG]·Cl(2), and [dMG]·Cl(4), the C^8−H vibrational frequency is almost the same as that in the isolated cation.

TABLE 4: Selected Partial Charges and Δ*q* from a NAO Analysis of [dMG]·Cl Series (Charges Are Calculated at the B3LYP/6-311++G//B3LYP/6-31++G** Level)[a]**

	cation	a	Δ*q*	b	Δ*q*	c	Δ*q*	d	Δ*q*
Cl		*−0.783*	*0.217*	*−0.773*	0.227	*−0.832*	*0.168*	*−0.710*	*0.290*
N1	−0.608	−0.642	*−0.034*	−0.617	−0.009	−0.613	−0.005	−0.611	−0.003
H1	0.425	0.457	*0.032*	0.412	−0.013	0.414	−0.011	0.412	−0.013
N2	−0.744	−0.759	−0.015	−0.742	0.002	−0.773	−0.029	−0.780	−0.036
H2a	0.410	0.439	*0.029*	0.380	*−0.030*	0.393	−0.017	0.388	−0.022
H2b	0.426	0.398	*−0.028*	0.412	*−0.014*	0.413	−0.013	0.407	−0.019
C8	0.318	0.278	*0.040*	0.294	−0.024	0.315	−0.003	0.355	*0.037*
H8	0.236	0.220	−0.016	0.222	−0.014	0.285	*0.049*	0.240	0.004

[a] Δ*q* denotes the electron difference between the ion pair and the isolated cation, i.e., Δ*q* = *q*(ion pair) − *q*(isolated cation/anion). (a) [dMG]·Cl(1); (b) [dMG]·Cl(2); (c) [dMG]·Cl(3); (d) [dMG]·Cl(4).

formation of the H···Cl bond is expected to weaken the associated C/N−H bond and produces a red shift and enhanced intensity of the related C/N−H stretching modes in IR spectra. The changes of the vibrational frequencies mainly depend on the position of the Cl anion. Generally, the vicinal bonds associated with H-bonds have significant changes in the vibrations for each of the ion pairs due to the influence of the H-bond, while the vibrational frequencies of the bonds remote to the H-bonds are expected to be changed slightly or unchanged.

In the case of [dMG]·Cl(1), there are significant red shifts (841.5 and 716.8 cm^{-1}, respectively) in the N^1−H and N^2−H stretching frequencies to 2737.5 and 3022.8 cm^{-1}, respectively (Table 3), and associated large increases in intensities. The stretching vibration of C^8−H does not change significantly. However, the symmetrical stretching vibration of N^2-H disappears and the C═O stretching vibration are red-shifted about 50 cm^{-1} and an associated small decreases in intensity, red shift of C═O stretching vibration is consistent with the elongation of the C═O bond distances. Here, the three new modes correspond to Cl anion bending in-plane (93.2 cm^{-1}) and stretching vibrations with small frequencies of 178.1 and 224.0 cm^{-1}. The intensities of three vibrations are weak. These changes of stretching vibration can be seen clearly in Figure 3.

Also, in the [dMG]·Cl(2) conformer, a great red shift for N^2−H^b vibration and an extreme increase in the intensity of N^2−H^b stretching vibration occur. In comparison with the symmetry vibration of N^2−H, the N^2−H^b stretching vibrational frequency is red-shifted by 1612.5 cm^{-1}. The significant increase in the vibrational intensity of N^2−H^b indicates that a strong H-bond is formed in this conformer. As mentioned above, the H-bond distance in this structure is 1.794 Å, which is the shortest H-bond among the four [dMG]·Cl structures.

In the [dMG]·Cl(3), the C^8−H stretching vibration is largely red-shifted (∼734.4 cm^{-1}) and the associated vibrational intensity is significantly enhanced, in agreement with the C^8−H bond length changes. The interaction of Cl anion with C^8−H does not apparently affect the remote N−H stretching vibration. In addition, the three additional vibrational frequencies related to the chloride are 53.7 (in-plane bending of chloride), 176.9, and 178.9 (stretching vibration toward C^8−H).

For the [dMG]·Cl(4) structure, there are slight red shifts for the symmetry and asymmetry stretching vibration of N^2−H (21.0 and 30.6 cm^{-1}, respectively), while the vibrational frequencies of C^8−H and N^1−H are blue-shifted by 27.6 and 18.4 cm^{-1}, respectively (Table 3), which is in agreement with the slight contraction of C^8−H and N^1−H bonds. Frequency analysis indicates that no H-bonding between Cl and C^8−H is formed in this conformer.

1.3.2. Charge Population and Bonding Analyses. NBO analyses of the four [dMG]·Cl structures were performed to describe the nature of the bonding interaction and occupations of the orbitals. Selected partial charges for the isolated cation and ion pairs are reported in Table 4. It is shown that the charge distribution in the cation of the ion pairs is qualitatively similar to that of the isolated cation, i.e., a significant negative charge on the nitrogen atoms, and most of the positive charge is located on the peripheral hydrogen and carbon atoms of guaninium ring except for the atom C^5. In addition, the electronic density of the cation of the ion pairs is increased due to the electron density shift from Cl anion to the cation. The largest electron transfer (∼0.29 *e*) from Cl anion to the guaninium is observed in [dMG]·Cl(4), while in [dMG]·Cl(3), the least electron transfer (∼0.18 *e*) is observed. However, when repositioning the Cl anion around the N−H bond in [dMG]·Cl(1) and [dMG]·Cl(2), the Cl anion transfers almost the same electron density to the cation (∼0.23 *e*). What is more, in four ion pairs, those atoms, except for atom H^b attached to N^2, that directly interact with the Cl anion become more positive and the associated nitrogen atoms become more negative, atom H^b becomes less positive. No correlation between the electron transferred and the relative stability of the ion pairs is observed.

TABLE 5: Primary Delocalization Interaction of [dMG]·Cl Series Occur from the Orbitals in the "From" Column to the Orbitals in the "To" Column[a]

	from	to	occupancy	$E(j)^2$/kcal/mol
[dMG]·Cl(1)	$Cl_{LP}(1)$	σ^*_{N1-H}	0.115(0.014)	2.43
	$Cl_{LP}(3)$	σ^*_{N1-H}		4.92
	$Cl_{LP}(4)$	σ^*_{N1-H}		26.77
	$Cl_{LP}(1)$	σ^*_{N2-H2a}	0.088(0.005)	1.59
	$Cl_{LP}(3)$	σ^*_{N2-H2a}		10.97
	$Cl_{LP}(4)$	σ^*_{N2-H2a}		15.26
[dMG]·Cl(2)	$Cl_{LP}(1)$	σ^*_{N2-H2b}	0.203(0.005)	5.99
	$Cl_{LP}(4)$	σ^*_{N2-H2b}		76.95
[dMG]·Cl(3)	$Cl_{LP}(1)$	σ^*_{C8-H}	0.120(0.011)	3.67
	$Cl_{LP}(4)$	σ^*_{C8-H}		40.34
	$Cl_{LP}(3)$	σ^*_{C11-H}		2.61
[dMG]·Cl(4)	$Cl_{LP}(1)$	π^*_{C8-N7}	0.561(0.497)	3.08
	$Cl_{LP}(4)$	π^*_{C8-N7}		47.49

[a] Values in/out parentheses are occupancies of the antibonding orbitals that in the isolated cation/ion pair.

On the other hand, according to the NBO analyses, it is obvious to observe that the charge transfer from Cl anion to the guaninium occurs through either a π-type interaction with π^*_{C-N} or through a σ-type interaction with σ^*_{C-H} or σ^*_{N-H} (the specific orbital and interaction are dependent on the position of Cl anion). This bonding interaction is apparent in a second-order perturbational analysis, Table 5. The electron occupancies of the selected antibonding orbital are presented in Table S2 of Supporting Information. For the structures ([dMG]·Cl(1), [dMG]·Cl(2), and [dMG]·Cl(3) in which the Cl anion remains in plane with guaninium ring, the greatest interactions are due to the lone pairs of electrons on the Cl anion interacting with the antibonding orbitals of σ^*_{C-H} or σ^*_{N-H} (i.e., $Cl^{lp} \rightarrow \sigma^*_{C-H}$

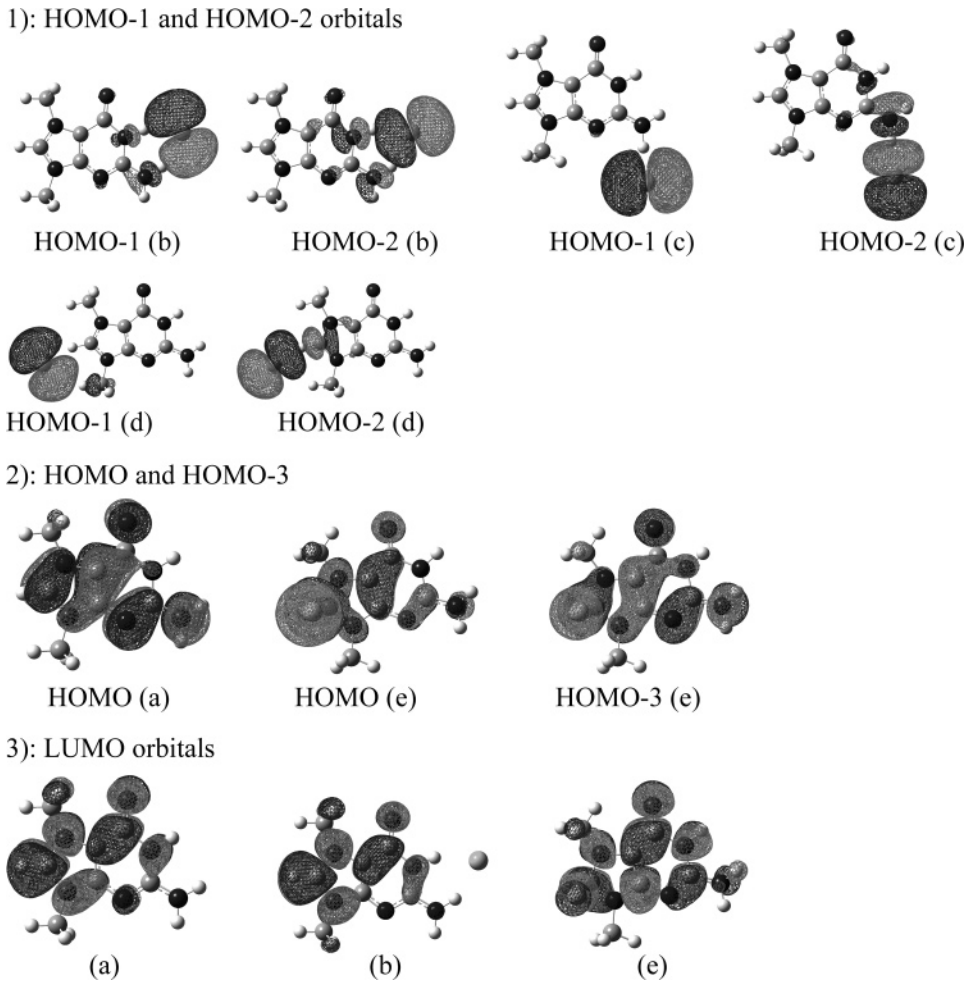

Figure 4. The HOMO, HOMO-1, HOMO-2, HOMO-3 and LUMO of the four ion pairs and the HOMO, HOMO-1 HOMO-2 and LUMO of the isolated cation. Isosurfaces calculated at 0.02. (a), (b), (c), (d), and (e) denote the isolated cation, [dMG]·Cl(1), [dMG]·Cl(2), [dMG]·Cl(3), and [dMG]·Cl(4), respectively.

or $Cl^{lp} \rightarrow \sigma^*_{N-H}$), which is associated with Cl···H H-bonding. The orbital interaction energies of these three conformers vary from 46 to 83 kcal/mol (Table 5, *E*(2)). The strong orbital interaction indicates that the electron transfer from the Cl anion to the cation occurs mainly via a σ-type interaction with either σ^*_{C-H} or σ^*_{N-H}. In [dMG]·Cl(3), there is an additional weak interaction from a lone pair of Cl to antibonding orbital σ^*_{C11-Ha}. The stabilization energy is 2.61 kcal/mol, indicating a weak H-bond between the Cl anion and $C^{11}-H^a$. However, for the [dMG]·Cl(4) ion pair, as expected, the charge transfer is mainly through $Cl^{lp} \rightarrow \pi^*_{C8-N7}$ interaction. The orbital interaction energies totally amount to ~50.57 kcal/mol. This interaction enhances the occupancy of π^*_{C8-N7} by 0.064 *e* as compared with that in the isolated cation (Table S2), which agrees with a lengthening of C^8-N^7 bond. On the other hand, large increases in the occupancy of the C/N−H antibonding orbitals ($\sigma^*_{C/N-H}$) are also observed (Table S2), which is associated with a weakening of the C/N−H bonds and the red shift of the C/N−H stretching frequencies described above, in comparison with the isolated cation (Table 3).

1.3.3. MOs. Figure 4 and Figure S1 display the highest-occupied molecular orbital (HOMO) and lowest-unoccupied molecular orbital (LUMO) of the cation and four [dMG]·Cl structures. For [dMG]·Cl(1), [dMG]·Cl(2), and [dMG]·Cl(3) in which Cl anion remains in plane with the guaninium ring, the HOMO is one of the three Cl anion atomic orbitals (pAOs, seen also in Figure S1), and the LUMO is essentially the cation LUMO. The similarity of the ion pair's LUMO to the isolated cation LUMO indicates small covalent interactions between the cation and the Cl anion. Additionally, it is observed that the HOMO-3 of the three structures is the cation HOMO (Figure S1). However, the HOMO-1 and HOMO-2 orbitals are somewhat different. In [dMG]·Cl(1), the HOMO-1 and the HOMO-2 have somewhat σ-type symmetry and exhibits the interaction between σ^*_{N1-H} and σ^*_{N2-Ha} antibonding orbitals and one of the p-type atomic orbital (Figure 4). However, in [dMG]·Cl-(3), HOMO-1 shows a slight interaction between one of the Cl pAOs with σ^*_{C11-Ha} of N9-methyl, in agreement with the structural depiction mentioned above. HOMO-2 shows σ-type symmetry and represents the interaction between σ^*_{N1-H} and one of the Cl pAOs. In [dMG]·Cl(2), HOMO-1 is also one of the p-type atomic orbitals of the Cl anion, but HOMO-2 exhibits $Cl^{pAO} \rightarrow \sigma^*_{N2-Hb}$ interaction. Hunt et al.[28] found the similar results on the examination of the electronic structure of the 1-butyl-3-methylimidazolium chloride ion pair, where the imidazolium can be thought of as the model of guaninium. They observed that the HOMO and HOMO-1 orbitals are two Cl pAOs, while HOMO-3 and LUMO are the same as the cation HOMO-3 and LUMO.

In the case of [dMG]·Cl(4) in which Cl anion lies above the C^8-H bond, the HOMO-1 and HOMO-2 are primary two Cl pAOs (Figure S1), however, the HOMO and HOMO-3 differ from those described above. The HOMO exhibits an interaction between one of Cl pAOs and the cation HOMO, while the HOMO-3 is essentially the interaction between the Cl pAOs and π_{C8-N7} of the cation (Figure 4). The LUMO of the [dMG]·

TABLE 6: Selected Wiberg Bond Index of the Isolated Cation and Four [dMG]·Cl Structures

	[dMG]$^+$	[dMG]·Cl(1)	[dMG]·Cl(2)	[dMG]·Cl(3)	[dMG]·Cl(4)
N^1-H	0.789	0.607	0.799	0.797	0.799
N^2-H^a	0.819	0.669	0.836	0.830	0.834
N^2-H^b	0.804	0.821	0.528	0.815	0.820
C^8-H	0.920	0.928	0.927	0.749	0.911
Cl···H−X		0.161	0.295	0.156	0.301
		(Cl···HN^1), 0.129(Cl···H^{a}N^2)			(Cl···C^8), 0.055(Cl···N^9), 0.079(Cl···N^7)

Cl(4) structure exhibits somewhat interaction between one of the Cl pAOs and the cation LUMO, especially $Cl^{pAO} \rightarrow \pi^*_{C8-N9}$ interaction. These interactions provide the evidence for the existence of Cl···π bond in the [dMG]·Cl(4) structure.

1.3.4. Wiberg Bond Index. To further confirm the essence of the bonding interaction between the Cl anion and the cation, the relative bond strength of the Cl···H bond of ion pairs was estimated using the Wiberg bond index analysis.[25e] The computed results are given in Table 6. It is seen from Table 6, for [dMG]·Cl(1), [dMG]·Cl(2), and [dMG]·Cl(3) in which Cl anion remains in plane with guaninium ring, the Wiberg bond index of Cl···H are in the range of 0.16−0.33, indicating partially covalent characters but to a small extent. According to the NBO analyses above, it can be deduced that these bond orders mainly arise from weak $Cl^{LP} \rightarrow \sigma^*_{C/N-H}$ hyperconjugative interactions. Correspondingly, formation of H-bonding decreases the bond index of the associated C/N−H bond. These results are in line with the lengthened bond distance and red shifts of C/N−H bond, suggesting a decrease in bond strength of the associated C/N−H bond. In [dMG]·Cl(4), the small bond orders between Cl···C^8, Cl···N^7, and Cl···N^1 indicates a small covalent character, which also clearly shows that the Cl anion could interact with both C8 and N7 simultaneously. Similarly, the $Cl^{LP} \rightarrow \pi^*_{C/N-H}$ interaction contributes to the small bond orders observed here. It also provides the evidence for our above depiction that the Cl anion transfers the electron density to the cation through the π-type interaction with π^*_{C8-N7}. Of course, formation of the Cl···π bond decreases the bond order of C^8−N^7 from 1.36 to 1.27. Additionally, the small covalent characters in the four structures seem to support that a strong ionic H-bond exists between Cl and the cation in the first three ion pairs and a strong ionic Cl···π bond in [dMG]·Cl(4) and thus lead to the large binding energies of these four ion pairs (energies range from 79 to 92 kcal/mol), since such large binging energies of the ion pairs could not be produced by weakly covalent H-bonds/Cl···π interaction.

2. [dMG]·*m*Cl Series (*m* = 2−4). *2.1. Geometrical Characteristics.* According to the acidity regions of the cation, it is deduced that each cation could be associated with one to four nearest Cl anions. Therefore, in this study, the interaction patterns of two to four Cl anions interacting with one cation were also chosen for investigation, as these systems have fewer atoms and thus to be easily calculated at a given level.

As for [dMG]·2Cl, two Cl anions were placed around the cation. After optimization, four stable structures ([dMG]·2Cl-(1.2), [dMG]·2Cl(1.3), [dMG]·2Cl(2.3), and [dMG]·2Cl(4.4)) were found (Figure 5). In the first three geometries, two anions remain essentially in a plane with the cation. They mainly H-bond with the cation N−H or/and C−H bonds. In [dMG]·2Cl(1.2), two chloride anions form three strong H-bonds with N^1−H and N^2−H^a and N^2−H^b, respectively [$r_{N1H\cdots Cl}$ = 2.011 Å, $A_{N1H\cdots Cl}$ = 161.1°; $r_{N2Ha\cdots Cl}$ = 2.356 Å, $A_{N2Ha\cdots Cl}$ = 146.5°; $r_{N2-Hb\cdots Cl}$ = 2.085 Å, $A_{N2-Hb\cdots Cl}$ = 175.4°]. In [dMG]·2Cl-(1.3), two Cl anions H-bond with the cation in the regions S1 and S3. They mainly form four hydrogen bonds, in which N^1−H···Cl (r_{N1}−H···Cl = 2.146 Å and A_{N1}−H···Cl = 153.1°), N^2−H^a···Cl (r = 2.096 Å and A = 153.8°) and C^8−H···Cl (r = 2.108 Å and A = 160.3°) are strong H-bonds; the last one is a weak interaction with C^{11}−H^a with $r_{C11-Ha\cdots Cl}$ = 2.729 Å. As for [dMG]·2Cl(2.3), two Cl anions are mainly associated with N^2−H^b and C^8−H, respectively. The H-bond lengths and bond angles are 1.947 Å and 161.8° for N^2−H^a···Cl; 2.087 Å and 161.1° for C^8−H···Cl. Additionally, there is a weak interaction between C^{10}−H and Cl with $r_{C10H\cdots Cl}$ = 2.722. As in the [dMG]·Cl series, formation of the Cl···H bond in these above three structures also lengthens the associated N/C−H bond of the cation. However, [dMG]·2Cl(4.4), in which two Cl anion lies in the front and back of the cation, respectively, is an exception. It is a nonplanar structure, and no strong H-bond is observed as in [dMG]·Cl(4). Two Cl anions weakly interact with C^8−H and C^{10}−H. Front-Cl anions position slightly closer to C^8 ($r_{C8\cdots Cl}$ = 2.886 Å), while back-Cl anions sit slightly closer to H on C^8 ($r_{C8H\cdots Cl}$ = 2.602 Å, Figure 5).

In the case of the [dMG]·3Cl series, four initial conformers are designed. After optimization, three stable structures are obtained (Figure 6.). [dMG]·3Cl(1.2.3) and [dMG]·3Cl(1.3.6) structures are planar structures, and five H-bonds are formed, in which four interactions with the ring N/C−H bond are strong, while the remaining interaction with methyl hydrogen is weak. The bond lengths and angles are shown in Figure 6. [dMG]·3Cl(2.3.5) is a nonplanar structure, in which four H-bonds are found. One is N^2−H^b···Cl with r = 2.165 Å and A = 144.6°. The second Cl anion interacts with C^8−H and C^{11}−H simultaneously ($r_{C8-H\cdots Cl}$ = 2.342 Å and $A_{C8-H\cdots Cl}$ =144.2°; $r_{C11-H\cdots Cl}$ = 2.528 Å and $A_{C11-H\cdots Cl}$ = 152.8°), and the third Cl anion interacts with C^{11}−H with bond length and angle of 2.420 Å and 163.8°.

For [dMG]·4Cl, the structure was preoptimized to a local minimum using the B3LYP/3-21G* level of theory. As is presented in Figure 6, four Cl anions interact with N−H and C−H bonds of the cation, mainly forming six H-bonds. Then,

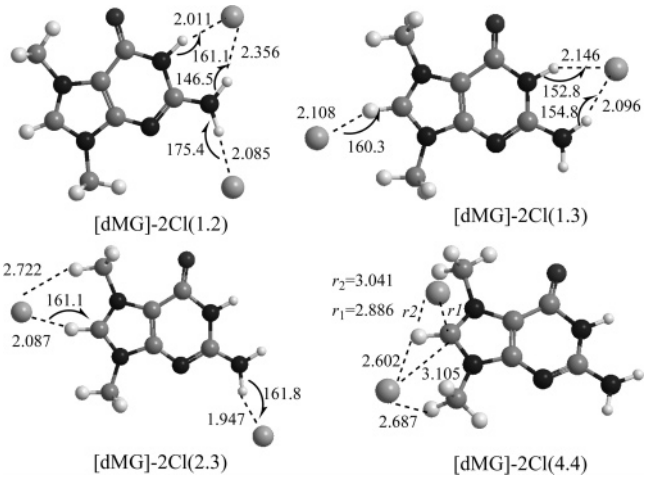

Figure 5. The interactions between two Cl anions and one cation, calculated at B3LYP/6-31+G**. All distances are in angstroms, and angles are in degrees.

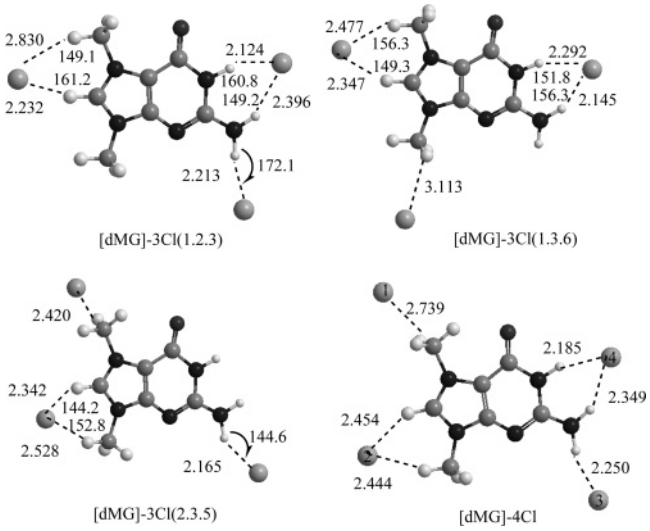

Figure 6. The interactions between three or four Cl anions an one cation. All are calculated at B3LYP/6-31+G** with the exception of [dMG]·4Cl, which is calculated at B3LYP/3-21G*. All distances are in angstroms, and angles are in degrees.

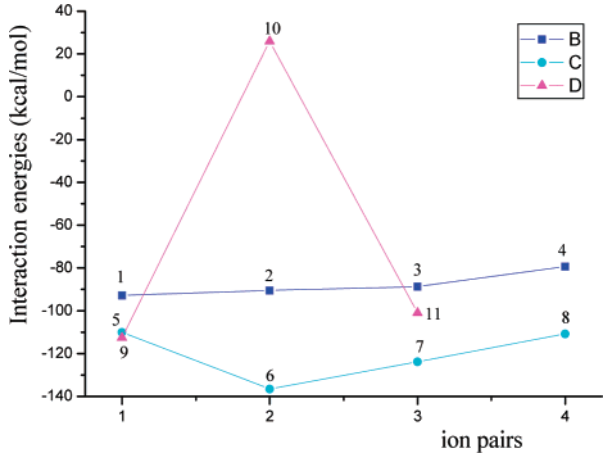

Figure 7. The interaction energies of [dMG]·*m*Cl series, which are calculated at B3LYP/6-3++G**//B3LYP/6-31+G**. (B) [dMG]·Cl series; (C) [dMG]·2Cl series; (D) [dMG]·3Cl series. Digits 1−11 denote the [dMG]·Cl(1), [dMG]·Cl(2), [dMG]·Cl(3), [dMG]·Cl(4), [dMG]·2Cl(1.2), [dMG]·2Cl(1.3), [dMG]·2Cl(2.3), [dMG]·2Cl(4.4), [dMG]·3Cl(1.2.3), [dMG]·3Cl(1.3.6), and [dMG]·3Cl(2.3.5), respectively.

this structure was further optimized at the B3LYP/6-31+G** level; however, it was found that one of the four Cl anions (Cl^1) leaves away from the cation, while Cl^2 moves toward C^8−H and C^{10}−H, but $C1^3$ and Cl^4 still interact with N−H. This suggests that each cation could interact with three nearest Cl anions in the gas phase but no more than three anions; this may be also truth in the condensed phase. The result is similar to the crystal structure of Emim chloride, in which each $Emim^+$ is associated with three nearest Cl anions.[15b]

2.2. Interaction Energies. In conjunction with [dMG]·Cl ion pairs, it can be seen that the absolute interaction energies magnitude of the [dMG]·*m*Cl ($m = 1-3$) strucutres are: [dMG]·2Cl(1.3) > [dMG]·2Cl(2.3) > [dMG]·3Cl(1.2.3) > [dMG]·2Cl-(4.4) ≈ [dMG]·2Cl(1.2) > [dMG]·3Cl(2.3.5) > [dMG]·Cl(1) > [dMG]·Cl(4) > [dMG]·Cl(3) > [dMG]·Cl(2) > [dMG]·3Cl-(1.3.6) (Table 2 and Figure 7). Generally, [dMG]·2Cl series have the larger binding energies than the other series, while the [dMG]·Cl series have the least binding energies with the exception of [dMG]·3Cl(1.3.6) (Figure 7). For example, [dMG]·2Cl(1.3) has a binding energy of −136.5 kcal/mol, ∼24 kcal/mol more stable than [dMG]·3Cl(1.2.3) and ∼44 kcal/mol more stable than [dMG]·Cl structures. Additionally, it is notable that the interaction energy of [dMG]·3Cl(1.3.6) is 25.8 kcal/mol. This means that in the gas phase this geometry would dissociate into component ions from a pure energetical point of view, neglecting kinetics.

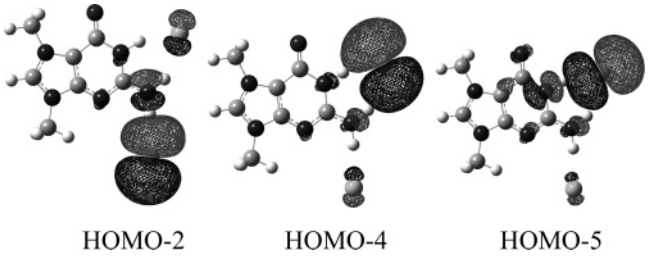

Figure 8. MOs of [dMG]·2Cl(1.2). Isosurfaces were calculated at 0.02.

The interaction energies also suggest that the cation does not appear to interact with the Cl anion individually in the condensed phase but appears to interact with two or three Cl anions in the regions N^1−H, N^2−H^a, and C^8−H. Among all of these interaction modes, H-bonding with two Cl anions, especially the interaction of two Cl anions with the cations N^1−H, N^2−H^a, and C^8−H ([dMG]·2Cl(1.3)), respectively, is the most possible.

2.3. Properties. The IR and electronic properties of [dMG]·*m*Cl series ($m = 2$ or 3) have also been analyzed. These properties are very similar to those of the [dMG]·Cl series. For example, three additional vibration modes appear as increasing one Cl anion in the ion pairs. The interaction of Cl anions with the cation red shifts the IR of the associated N−H and/or C−H bond and enhances the intensity of the vibration significantly (Table S3). And also, frequency analysis suggests that there is no strong H-bonding between Cl and C^8−H in [dMG]·2Cl(4.4). These results can be also verified by NBO analyses. As Table S4 presented, the primary orbital interactions between the cation and the anions are $Cl^{lp} \rightarrow \sigma^*_{N-H}$ and (or) $Cl^{lp} \rightarrow \sigma^*_{C-H}$. These interactions increase the occupation of σ^*_{N-H} and (or) σ^*_{C-H} and thus weaken the associated N−H and/or C−H bonds, of course, decreasing the bond index of the associated N−H and/or C−H bond (Table S5). Unlike the other [dMG]·*m*Cl structures, the orbital interaction of [dMG]·2Cl(4.4) is different, in which the greatest orbital interaction is $Cl^{lp} \rightarrow \pi^*_{C-N}$ and not the $Cl^{lp} \rightarrow \sigma^*_{N-H}$ and (or) $Cl^{lp} \rightarrow \sigma^*_{C-H}$ interaction. This implies that there is a Cl···π interaction but no strong H-bond in this structure, which is in line with the geometrical characters and frequency analyses described above. Like the [dMG]·Cl series, these interactions also suggest that the charge transfer from Cl anion to the guaninium cation occurs mainly through either a π-type interaction with π^*_{C-N} or through a σ-type interaction with σ^*_{C-H} or σ^*_{N-H}. The total charge-transfer values of the Cl anions in [dMG]·2Cl and [dMG]·3Cl series are almost the same as that in the [dMG]·Cl series (Table S4), demonstrating that the charge-transfer values are little related to the number of the anions. Additionally, the Cl···H bond orders in [dMG]·2Cl and [dMG]·3Cl series are small (Table S5), which also indicates a weak covalent H-bond and suggests a strong ionic Cl···H bond or Cl···π bond.

As for the MOs of [dMG]·2Cl and [dMG]·3Cl series, there is also some similarity to [dMG]·Cl series. The detailed orbital information is presented in Figures 8 and 9 and Figures S2 and S3 in the Supporting Information. As MOs in the [dMG]·Cl series, the first 3m highest-occupied orbitals (from HOMO to HOMO-(3m − 1)) of the [dMG]·mCl series except [dMG]·2Cl(4.4) are related to Cl pAOs. These MOs exhibit either one

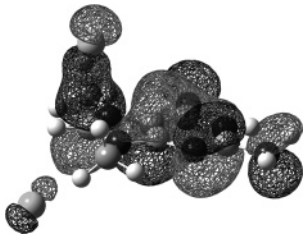

Figure 9. HOMO-6 orbital of [dMG]·2Cl(4.4). Isosurfaces were calculated at 0.02.

of the Cl pAOs or the interaction of Cl pAO with σ^*_{N-H} and/or σ^*_{C-H} antibonding orbitals (Figures 8, S2, and S3). The HOMO-3m and LUMO orbitals are the same as those in the isolated cations. This suggests that there is weak covalent character in these structures. For [dMG]·2Cl(4.4), in which two Cl anions lie in the front and the back of guaninium, the MOs are similar to those of [dMG]·Cl(4). The first six highest-occupied orbitals are pAOs of two Cl anions. HOMO-6 shows the interaction of one of the Cl pAOs with the cation HOMO (Figure 9). All of the similarities described above suggest that the number of the counterions around the cation has little effect on the bonding interaction and the electronic properties such as charge transfer, MOs, and so on. This also indicates that the study on the properties of [dMG]·Cl is enough to illustrate the properties associated with bonding interaction and electronic properties of the larger cluster built from one cation with several counterions from another view of the point.

3. [2dMG]·Cl Series. *3.1. Geometries and Interaction Energies.* The interaction of two cations with one Cl anion gives four stable structures (Figure 10). In [2dMG]·Cl-1, two cations are mutually perpendicular (side view in Figure 10) and essentially centrosymmetric to the Cl anion. The anion bridges two cations and hydrogen bonds with four N^1-H and N^2-H^a bonds of the two cations ($r_{Cl\cdots HN1} = 2.235$ Å and $A_{Cl\cdots HN1} = 153.7°$; $r_{N2Ha\cdots Cl} = 2.246$ Å and $A_{N2Ha\cdots Cl} = 151.4°$). In [2dMG]·Cl-2, two cations are nonplanar. Cl anion inteacts with N^1-H and N^2-H^a of one cation (with $r_{Cl\cdots HN1} = 1.952$ Å and $A_{Cl\cdots HN1} = 166.1°$; $r_{N2Ha\cdots Cl} = 2.165$ Å and $A_{N2Ha\cdots Cl} = 160.2°$) and N^2-H^a of another cation (with $r_{N2Ha\cdots Cl} = 2.165$ Å and $A_{N2Ha\cdots Cl} = 160.2°$). Additionally, the carbonyl oxygen atom of one cation hydrogen bonds with N^1-H of another cation with $r = 1.872$ Å and $A = 162.5°$. As for [2dMG]·Cl-3 and [2dMG]·Cl-4, two cations and Cl anion are in a plane (side view in Figure 10). In these two conformers, Cl interacts with N^1-H and N^2-H^a of one cation and C^8-H and N^7/N^9-methyl hydrogen atom of another cation. Again, as observed in the [dMG]·*m*Cl series, formation of Cl···H bond also lengthens the associated N/C−H bond by different values.

Among these four structures, [2dMG]·Cl-1 has the largest interaction energy (about −130.7 kcal/mol), while the other three structures have almost the same interaction energies, about 3.5 kcal/mol less stable than [2dMG]·Cl-1. This suggests that [2dMG]·Cl-1 is the most possible structure when two cations interact with one Cl anion.

3.2. Properties. To compare with the [dMG]·*m*Cl series, the IR spectra and electronic properties of [2dMG]Cl have also been studied. As anticipated, interaction of Cl anion with two cations red shifts the associated N/C−H bonds (Table S6) and increases the occupation of the associated N/C−H antibonding orbitals (Table S7) and thus weakens the corresponding bond indexes (Table S8). Small covalent Cl···H bond order also indicates a weak covalent H-bond and suggests a strong ionic H-bond. Additionally, inspection of the orbital interactions in Table S7 also reveals that the charge transfers from Cl to the cation mainly via a σ-type interaction with σ^*_{N-H} or (and) σ^*_{C-H} orbitals. What is more, it is interesting to find that the charge transfer is not higher than that in the [dMG]·*m*Cl series, although there are two cation could accept the charge. The charge on Cl anions and antibonding orbitals are listed in Table S7 of Supporting Information.

The MOs of [2dMG]Cl-1 are different from those in the [dMG]·*m*Cl series. In this structure, each orbital exhibit centrosymmetric to the Cl anion. What is more, the orbitals appear in pairs, for example, HOMO and HOMO-1 are the same (Figure 11), while HOMO-2 is the same as HOMO-3, and HOMO-5 is the same as HOMO-6, etc. (Figure S4). The first four highest-occupied orbitals (HOMO to HOMO-3) display interaction between one of the Cl p-type orbitals and the cation HOMO. HOMO-4 exhibits one of the Cl pAOs interactions with two σ^*_{N1-H} and two σ^*_{N2-Ha} of the two cations. This interaction corresponds to the Cl···H bond, which is consistent with the geometrical character and the orbital interaction described above. Interestingly, it is found that HOMO-5 (also HOMO-6) is the two cation HOMO-1 orbitals combined simply, but no interactions exist between these two cation orbitals. Similarly, LUMO (also LUMO+1) is the two cation LUMO orbitals combined simply. In the other three structures, the HOMO-1 and HOMO-2 display the interaction of Cl pAO with the associated σ^*_{N-H} or (and) σ^*_{C-H} orbitals. Additionally, like MOs in the [dMG]·Cl series, HOMO-3 and HOMO-4 are one of the cation HOMOs. Similarly, the LUMO and LUMO+1 are one of the cation LUMOs. This also indicates that there is little covalent character between the cation and the anion, which is in agreement with the bond order analysis.

4. Future Prospects for Molecular Dynamics. It is well-known that in bulk ILs, energetics of each ion is strongly influenced by the rest of the liquid. This is also the case for the vibration of H-bond in the condensed state. It is estimated that free energy of solvation of each ion ranges from −80 to −100 kcal/mol for imidazolium-based ILs,[31] which should be comparable with (or higher than) free energy of hydration.[32] Thus, the prediction of thermophysical properties or fundamental properties (such as melting points and dielectric constants) of ILs is important for furture application. However, to date, molecular modeling for the energetical or qualitative prediction of ILs is limited.[31−33] This reflects difficulties in developing appropriate force fields for ILs and performing molecular simulation with proper treatment of longe-range electrostatics. Furthermore, the extent to which a molecular simulation accurately predicts thermophysical properties depends on the quality of the force field used to describe the intramolecular and intermolecular energetics. Fortunately, several groups have recently made a significant contribution to the construction of such force fields, such as Jordan et al.,[34] Jorgensen et al.,[35] and Kollman et al.[36]

With regard to the current newly designed IL, the present calculation can be regarded as the foundation of the future molecular modeling, since some force fields such as the OPLS-AA/AMBER usually employ quantum calculations to generate geometrical and conformational parmeters that are not available for the molecules under investigation in these force fields.[35,36] Recently, Mavri et al.[37] have first performed the vibrational analysis of the condensed phase using Carr−Parrinello molecular dynamics study in conjunction with solving the vibrational Schrödinger equation for the snapshots, which provides a new method for the vibrational analysis of the condensed phase. All of these light up the hope for future molecular simulation of

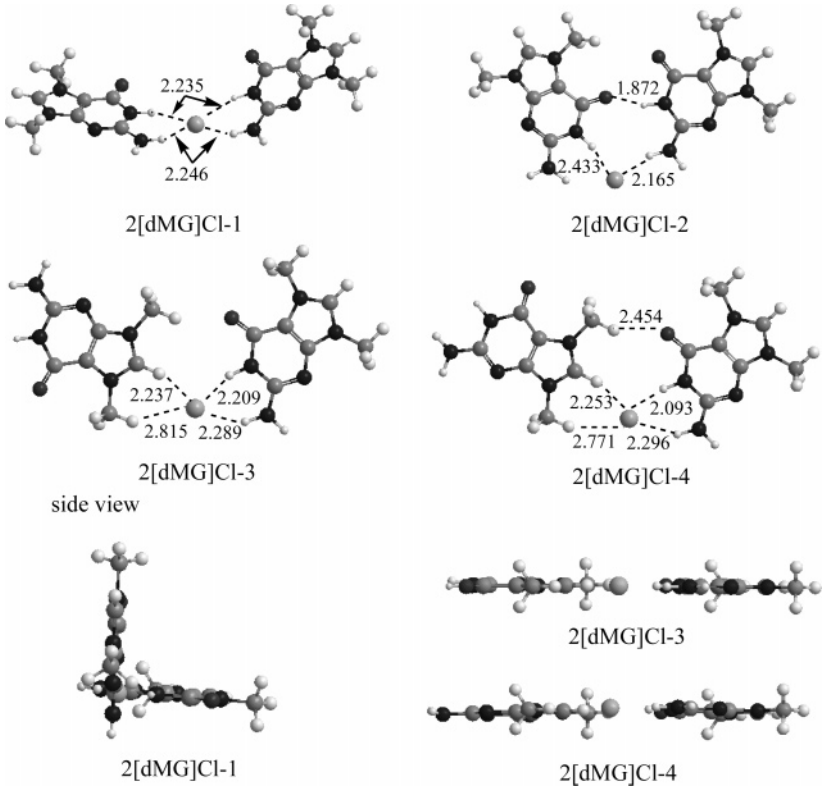

Figure 10. Interactions of two catons with one Cl anion. All are calculated at B3LYP/6-31+G*. All distances are in angstroms, and angles are in degrees.

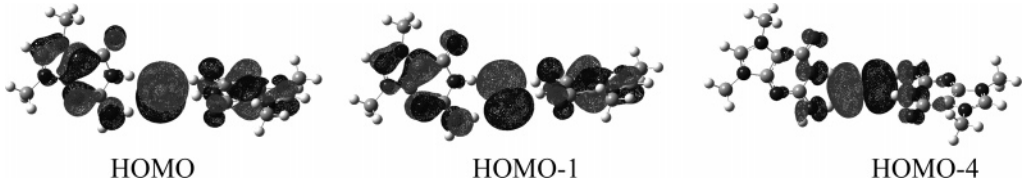

Figure 11. MOs of [2dMG]·Cl. Isosurfaces were calculated at 0.02.

N7,N9-dimethylguaninium chloride IL, in spite of the absence of the experimental data.

Summary and Conclusions

In this paper, a new assumption using N7,N9-dimethylguaninium chloride as an IL is provided. To investigate the structural and electronic properties of guaninium chloride and bridge the relationship between the structure and properties, a series of [dMG]·*m*Cl ($m = 1-4$) structures and [2dMG]·Cl structures have been studied. On the base of our calculations, it is found that:

(1) In the cation, there are mainly four favorable regions (S1, S2, S3, and S4) for Cl anions. The cation(s) and the anion(s) form 15 stable conformers in these regions. The guaninium cation could interact with one to three Cl anions but no more than three nearest anions. And one Cl anion could H-bond with two cations. Among these structures, one cation H-bonds with two Cl anions, and the interaction of the two Cl anions with the cations N^1-H, N^2-H^a, and C^8-H ([dMG]·2Cl(1.3)), respectively, is the most possible. Two cations N^1-H and N^2-H^a interacting with one Cl anion ([2dMG]·Cl-1) is the next possible structure.

(2) High interaction energies of the ion pairs may imply high viscosity, negligible vapor pressure, and a high melting point. The binding energies of [dMG]·Cl are slightly higher or comparable to those of the IL based on the imidazolium,[26,28] which may suggest that the physical properties of [dMG]Cl including melting point is comparable to that of imidazolium chloride based IL.

(3) Frequency analyses of each conformer explain the origin of H-bonding character and suggest that there is no strong H-bond in the structures in which Cl anion locates in the front or/and the back of the cation.

(4) NBO analyses suggest that the electron transfer from the Cl anion to the cation occurs mainly through either the $Cl^{lp} \rightarrow \sigma^*_{C8-H}$, $Cl^{lp} \rightarrow \sigma^*_{N-H}$, or $Cl^{lp} \rightarrow \pi^*_{C8-N7}$ interactions. This electron transfer has nothing to do with the number of the counterions around the cation or the anion. The interactions between Cl anion(s) and the cation(s) produce a small bond order of Cl···H/Cl···π bond, indicating that the Cl···H/Cl···π bond exhibits a weak covalent character and suggesting a strong ionic Cl···H/Cl···π bond.

(5) The components of the MOs are little related to the counterions around the cation(s) or the anion(s). For example, the HOMO-3m and LUMO of the [dMG]·*m*Cl series and LUMO of the [2dMG]·Cl series are the same as those of the isolated cations.

In summary, the interaction of one cation with one to four Cl anions and two cations with one anion were studied in detail. Although the gas-phase calculation may be different from the condensed states, the results obtained here may allow us to speculate about the structural and electronic properties of the

ILs and thereby the physical properties. As is known, many of the physical properties are determined by molecular interactions, such as the viscosity interaction energy and melting point interaction energy. All of the information obtained above could be the fundamental base for further studies on the simulation and experiment later.

Acknowledgment. This work is supported by NSFC (20573063, 20633060) to Y.B., NIH (Grant No. GM62790) to R.I.C., NCET and Shandong-NSF (Z2003B01) to Y.B. A part of calculations were performed on the HPCC at Shandong University. The author (Y.B.) also thanks Prof. Yi Hu for his help in calculations.

Supporting Information Available: Detailed geometry parameters, orbital interactions, bond indexes, and MOs of each structure. This material is available free of charge via the Internet at http://pubs.acs.org.

References and Notes

(1) Welton, T. *Chem. Rev.* **1999**, *99*, 2071−2083.
(2) Visser, A. E.; Swatloski, R. P.; Rogers, R. D. *Green Chem.* **2000**, *2*, 1−4.
(3) Chun, S.; Dzyuba, S. V.; Bartsch, R. A. *Anal. Chem.* **2001**, *73*, 3737.
(4) van Rantwijk, F.; Lau, R. M.; Sheldon, R. A. *Trends Biotechnol.* **2003**, *21*, 121.
(5) Liu, W. M.; Ye, C. F.; Gong, Q. Y.; Wang, H. Z.; Wang, P. *Tribol. Lett.* **2002**, *13*, 81.
(6) Hayashi, S.; Hamaguchi, H. *Chem. Lett.* **2004**, *33*, 1590.
(7) Hayashi, S.; Saha, S.; Hamaguchi, H. *IEEE Trans. Magn.* **2006**, *42*, 12.
(8) Earle, M. J.; Katdare, S. P.; Seddon, K. R. *Org. Lett.* **2004**, *6*, 707−710.
(9) Lancaster, N. L.; Welton, T.; Young, G. B. *J. Chem. Soc., Perkin Trans.* **2001**, *2*, 2267−2270.
(10) Lancaster, N. L.; Salter, P. A.; Welton, T.; Young, G. B. *J. Org. Chem.* **2002**, *67*, 8855−8861.
(11) Fischer, T.; Sethi, A.; Welton, T.; Woolf, J. *Tetrahedron Lett.* **1999**, *40*, 793−796.
(12) Cammarata, L.; Kazarian, S. G.; Salter, P. A.; Welton, T. *Phys. Chem. Chem. Phys.* **2001**, *3*, 5192−5200.
(13) Aggarwal, A.; Lancaster, N. L.; Sethi, A. R.; Welton, T. *Green Chem.* **2002**, *4*, 517−520.
(14) Wilkes, J. S.; Levisky, J. A.; Wilson, R. A.; Hussey, C. L. *Inorg. Chem.* **1982**, *21*, 1263−1264.
(15) (a) Singh, R. P.; Verma, R. D.; Meshri, D. T.; Shreeve, J. M. *Angew. Chem., Int. Ed*. **2006**, *45*, 3584−3601 and references therein. (b) Dymek, C. J.; Grossie, D. A.; Fratini, A. V.; Adams, W. W. *J. Mol. Struct.* **1989**, *213*, 25.
(16) Fukumoto, K.; Yoshizawa, M.; Ohno, H. *J. Am. Chem. Soc.* **2005**, *127*, 2398−2399.
(17) Forsyth, S. A.; Pringle, J. M.; MacFarlane, D. R. *Aust. J. Chem.* **2004**, *57*, 113−119.
(18) Anderson, J. L.; Armstrong, D. W. *Anal. Chem.* **2003**, *75*, 4851−4858.
(19) Anderson, J. L.; Ding, R.; Ellern, A.; Armstrong, D. W. *J. Am. Chem. Soc.* **2005**, *127*, 593−604.
(20) Tsuzuki, S.; Tokuda, H.; Hayamizu, K.; Watanabe, M. *J. Phys. Chem. B* **2005**, *109*, 16474−16481.
(21) (a) Buckingham, A. D.; Fowler, P. W.; Hutson, J. M. *Chem. Rev.* **1988**, *88*, 963. (b) Chalasinski, G.; Szczesniak, M. M. *Chem. Rev.* **2000**, *100*, 4227.
(22) (a) Dunning, T. H., Jr. *J. Phys. Chem. A* **2000**, *104*, 9062. (b) Tsuzuki, S.; Luthi, H. P. *J. Chem. Phys.* **2001**, *114*, 3949. (c) Tsuzuki, S.; Honda, K.; Uchimaru, T.; Mikami, M.; Tanabe, K. *J. Am. Chem. Soc.* **2002**, *124*, 104.
(23) (a) Meng, Z.; Dölle, A.; Carper, W. R. *THEOCHEM* **2002**, *585*, 119. (b) Rappe, A. K.; Bernstein, E. R. *J. Phys. Chem. A* **2000**, *104*, 6117.
(24) Frisch, M. J.; Trucks, G. W.; Schlegel, H. B.; Scuseria, G. E.; Robb, M. A.; Cheeseman, J. R.; Montgomery, J. A., Jr.; Vreven, T.; Kudin, K. N.; Burant, J. C.; Millam, J. M.; Iyengar, S. S.; Tomasi, J.; Barone, V.; Mennucci, B.; Cossi, M.; Scalmani, G.; Rega, N.; Petersson, G. A.; Nakatsuji, H.; Hada, M.; Ehara, M.; Toyota, K.; Fukuda, R.; Hasegawa, J.; Ishida, M.; Nakajima, T.; Honda, Y.; Kitao, O.; Nakai, H.; Klene, M.; Li, X.; Knox, J. E.; Hratchian, H. P.; Cross, J. B.; Bakken, V.; Adamo, C.; Jaramillo, J.; Gomperts, R.; Stratmann, R. E.; Yazyev, O.; Austin, A. J.; Cammi, R.; Pomelli, C.; Ochterski, J. W.; Ayala, P. Y.; Morokuma, K.; Voth, G. A.; Salvador, P.; Dannenberg, J. J.; Zakrzewski, V. G.; Dapprich, S.; Daniels, A. D.; Strain, M. C.; Farkas, O.; Malick, D. K.; Rabuck, A. D.; Raghavachari, K.; Foresman, J. B.; Ortiz, J. V.; Cui, Q.; Baboul, A. G.; Clifford, S.; Cioslowski, J.; Stefanov, B. B.; Liu, G.; Liashenko, A.; Piskorz, P.; Komaromi, I.; Martin, R. L.; Fox, D. J.; Keith, T.; Al-Laham, M. A.; Peng, C. Y.; Nanayakkara, A.; Challacombe, M.; Gill, P. M. W.; Johnson, B.; Chen, W.; Wong, M. W.; Gonzalez, C.; Pople, J. A. *Gaussian 03*, revision C.02; Gaussian, Inc.: Wallingford, CT, 2004.
(25) (a) Reed, A.; Curtiss, L. A.; Weinhold, F. *Chem. Rev.* **1988**, *88*, 899. (b) Reed, A.; Weinhold, F.; Curtiss, L. A.; Pochatko, D. *J. Chem. Phys.* **1986**, *84*, 5687. (c) Reed, A.; Weinhold, F. *J. Chem. Phys.* **1985**, *83*, 1736. (d) Reed, A.; Weinstock, R. B.; Weinhold, F. *J. Chem. Phys.* **1985**, *83*, 735. (e) Wiberg, K. B. *Tetrahedron* **1968**, *24*, 1083−1096
(26) Kossmann, S.; Thar, J.; Kirchner, B.; Hunt, P. A.; Welton, T. *J. Chem. Phys.* **2006**, *124*, 174506.
(27) (a) Hunt, P. A.; Gould, I. R. *J. Phys. Chem. A* **2006**, *110*, 2269−2282. (b) Turner, E. A.; Pye, C. C.; Singer, R. D. *J. Phys. Chem. A* **2003**, *107*, 2277−2288.
(28) Hunt, P. A.; Kirchner, B.; Welton, T. *Chem.−Eur. J.* **2006**, *12*, 6762−6775.
(29) Dykstra, C. E. *Acc. Chem. Res.* **1988**, *21*, 355 and references therein.
(30) (a) Scheiner, S. *Hydrogen Bonding*; Oxford University Press: New York, 1997. (b) Desiraju, G. R.; Steiner, T. *The Weak Hydrogen Bond*; Oxford University Press: Oxford, 1999.
(31) Krossing, I.; Slattery, J. M.; Daguenet, C.; Dyson, P. J.; Oleinikova, A.; Weingärtner, H. *J. Am. Chem. Soc.* **2006**, *128*, 13427−13434.
(32) Jorgensen, W. L.; Ulmschneider, J. P.; Tirado-Rives, J. *J. Phys. Chem. B* **2004**, *108*, 16264−16270.
(33) (a) Canongia Lopes, J. N.; Deschamps, J.; Pádua, A. A. H. *J. Phys. Chem. B* **2004**, *108*, 2038−2047. (b) Canongia Lopes, J. N.; Pádua, A. A. H. *J. Phys. Chem. B* **2006**, *110*, 19586−19592.
(34) Jordan, P. C.; Maaren, P. J.; Mavri, J.; Spoel, D.; Berendsen, H. J. C. *J. Chem. Phys.* **1995**, *103*, 2272−2284.
(35) (a) Damm, W.; Tirado-Rives, F. J.; Jorgensen, W. L. *J. Comput. Chem.* **1997**, *18*, 1955−1970. (b) Jorgensen, W. L.; Maxwell, D. S.; Tirado-Rives, J. *J. Am. Chem. Soc.* **1996**, *118*, 11225−11236. (c) Jorgensen, W. L.; Tirado-Rives, J. *J. Am. Chem. Soc.* **1988**, *110*, 1657−1666. (d) Kaminski, G.; Duffy, E. M.; Matsui, T.; Jorgensen, W. L. *J. Phys. Chem.* **1994**, *98*, 13077−13082.
(36) (a) Cornell, W. D.; Cieplak, P.; Bayly, C. I.; Gould, I. R.; Merz, K. M., Jr.; Ferguson, D. M.; Spellmeyer, D. C.; Fox, T.; Caldwell, J. W.; Kollman, P. A. *J. Am. Chem. Soc.* **1995**, *117*, 5179−5197. (b) Weiner, P. K.; Kollman, P. A. *J. Comput. Chem.* **1981**, *2*, 287−303. (c) Weiner, S. J.; Kollman, P. A.; Case, D. A.; Singh, U. C.; Ghio, C.; Alagona, G.; Profeta, S., Jr. *J. Am. Chem. Soc.* **1984**, *106*, 765−784. (d) Weiner, S. J.; Kollman, P. A.; Nguyen, D. T.; Case, D. A. *J. Comput. Chem.* **1986**, *7*, 230−252.
(37) Jezierska, A.; Panek, J. J.; Koll, A.; Mavri, J. *J. Chem. Phys.* **2007**, *126*, 205101.